

LossAgent: Towards Any Optimization Objectives for Image Processing with LLM Agents

Bingchen Li Xin Li[†] Yiting Lu Zhibo Chen

University of Science and Technology of China

{lbc31415926, luyt31415}@mail.ustc.edu.cn, {xin.li, chenzhibo}@ustc.edu.cn

Abstract

We present the first loss agent, dubbed *LossAgent*, for low-level image processing tasks, e.g., image super-resolution and restoration, intending to achieve any customized optimization objectives of low-level image processing in different practical applications. Notably, not all optimization objectives, such as complex hand-crafted perceptual metrics, text description, and intricate human feedback, can be instantiated with existing low-level losses, e.g., MSE loss, which presents a crucial challenge in optimizing image processing networks in an end-to-end manner. To eliminate this, our *LossAgent* introduces the powerful large language model (LLM) as the loss agent, where the rich textual understanding of prior knowledge empowers the loss agent with the potential to understand complex optimization objectives, trajectory, and state feedback from external environments in the optimization process of the low-level image processing networks. In particular, we establish the loss repository by incorporating existing loss functions that support the end-to-end optimization for low-level image processing. Then, we design the optimization-oriented prompt engineering for the loss agent to actively and intelligently decide the compositional weights for each loss in the repository at each optimization interaction, thereby achieving the required optimization trajectory for any customized optimization objectives. Extensive experiments on three typical low-level image processing tasks and multiple optimization objectives have shown the effectiveness and applicability of our proposed *LossAgent*.

1. Introduction

With the revolutionary advancements in deep learning technology, low-level image processing tasks, e.g., image super-resolution and restoration, have garnered increasing interest from researchers. Typically, low-level image processing tasks are optimized with the commonly-used loss function, such as MSE and L1 Losses, in an end-to-end manner, to

improve the objective quality [8, 11, 21, 22, 52, 60] or perceptual quality [6, 7, 48, 58, 59, 62]. However, optimizing models using a single optimization objective falls short of meeting real-world needs. For example, in image super-resolution, we desire the super-resolved images to not only restore the ground truth at the pixel level but also to appear natural without artificial textures or visually distracting artifacts [17]. To address this, some researchers have introduced the combination of multiple loss functions [17, 46–48, 62] (e.g., GANs) to train networks, enabling the optimized models to satisfy multiple optimization objectives. Nevertheless, this approach requires the loss functions corresponding to optimization objectives to be differentiable and suitable for training. Consequently, some advanced image quality assessment (IQA) metrics, which align more closely with human visual perception, are not differentiable and thus cannot be directly utilized for end-to-end network optimization.

Recently, large language models (LLMs) such as GPT series [4, 33] and LLaMA series [29, 35, 43], have shown promising reasoning and understanding capabilities. This has also catalyzed the trend of utilizing LLMs as intelligent agents [12, 24, 38, 39], especially in the field of embodied AI [15, 32, 37, 54]. By providing the agent with the environment information, predefined settings, rules, external feedback, and a set of optional actions, it can leverage its powerful reasoning capabilities to generate outputs that meet customized requirements, such as tool selection [36, 38], action decisions [56], programming [15, 41], etc.

Inspired by this series of works, we propose the first loss agent, dubbed *LossAgent*, for low-level image processing, enabling any customized optimization objectives of the image processing network for multiple practical applications. To achieve this, we introduce the pre-trained large language model (LLM), *i.e.*, LLaMA-3 [29] as the loss agent to control the optimization trajectory for different objectives. In the optimization process, an intuitive strategy is to exploit the expected optimization objective as the loss function to guide the optimization of image processing networks. However, not all optimization objectives can assist this, such as the complex hand-crafted optimization objective, textual

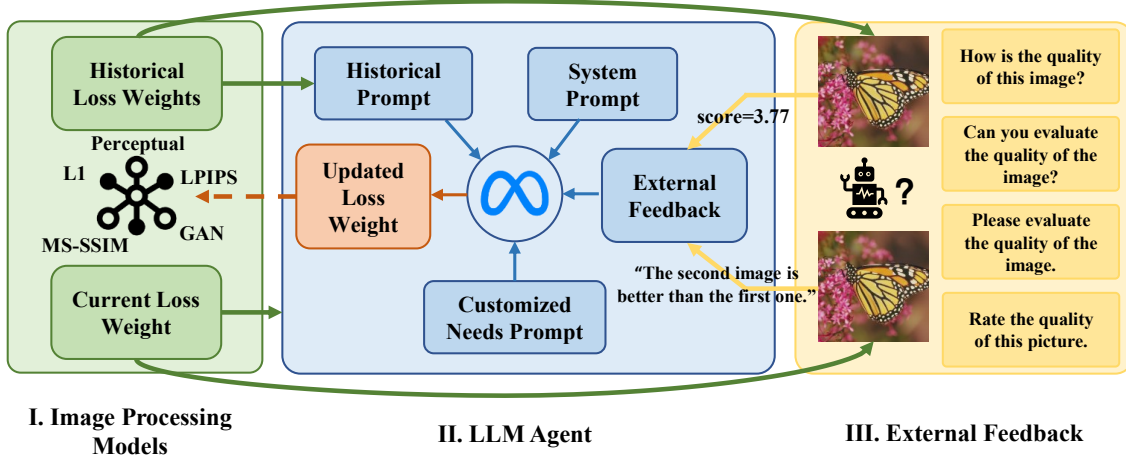


Figure 1. During the training of image processing models (Part I), the loss agent (Part II) gathers feedback from various optimization objectives (Part III). Combining this feedback with historical information, the LLM leverages its powerful reasoning capabilities to determine the optimal loss weights for the subsequent optimization phase of the image processing models (Part I).

description, and human feedback, since they cannot be differentiable for end-to-end optimization. To solve the problem, we propose the compositional loss repository, which collects existing popular loss functions supported for low-level image processing, and utilize our proposed LossAgent to adaptively and actively assign the weights for each loss at each iteration period based on external environments to achieve customized optimization trajectory toward the required optimization objective. In this process, we carefully design the optimization-oriented prompt engineering, which constructs the prompt templates to guide the LLM to understand the current optimization states, trajectory, and objectives, thereby achieving accurate loss weights planning.

To fully utilize the reasoning capabilities of LLM, the agent receives input of all weights of the model from the beginning of the training phase to the current stage. This enables the LossAgent to smoothly and automatically optimize the image processing model toward predefined optimization objectives through the analysis of historical weights, inference from external feedback, and following customized instructions.

Overall, the LossAgent possesses the following core features:

- LossAgent is capable of obtaining feedback from non-differentiable optimization objectives and leveraging the model’s powerful reasoning capabilities to convert this feedback into a composition of loss weights for training, thereby enabling the model to be optimized in an end-to-end manner toward any optimization objectives.
- LossAgent enjoys a high degree of flexibility. Leveraging its powerful reasoning capabilities, the agent can update loss weights fully automatically. Additionally, due to its ability to follow instructions, it can also receive feedback

from external environments during the training process to pursue customized needs.

- LossAgent exhibits high scalability. As depicted in Figure 1, our AgentLoss can be extended to various low-level image processing tasks and multiple different optimization objectives, even if they are not differentiable, which has been proven in the experimental parts.

2. Related Works

2.1. Image Processing

Image processing consists of a broad spectrum of tasks, including image restoration [11, 22, 34], image enhancement [45, 49, 58], and image super-resolution [6, 7, 48, 59, 62]. In low-level image processing tasks, pioneering works [9, 23, 64] focus primarily on optimizing fidelity-wise metrics, such as PSNR and SSIM, through L1 or MSE loss functions. However, models optimized by these metrics tend to generate over-smoothed results [17]. To mitigate this problem, works [17, 47, 48, 62] leverage generative adversarial networks (GANs) to enable the SR network to learn the distribution of real-world high-quality images. By introducing a weighted combination of VGG perceptual loss [17, 40] and GAN loss, GAN-based works [47, 48, 62] are well optimized for human perception objectives. More recently, transformer-based [6, 7, 22] and diffusion-based works [11, 25, 52] further improve the performance on aforementioned optimization objectives.

However, despite the revolution of network structures and loss function designs, optimization trajectories of image processing models have become relatively fixed. While there is a strong demand for advanced image quality assessment (IQA) metrics [62], many recently developed IQA metrics [50, 51, 57] cannot be utilized as optimization ob-

jectives due to their non-differentiable nature. In this paper, we tackle this challenge by introducing an LLM-based loss agent. This agent is capable of bridging any customized optimization objectives with the combination of loss function weights, allowing for the optimization of image processing models in an end-to-end manner.

2.2. LLM Agents

With the development of data science and computing resources, numerous large language models (LLMs) [4, 20, 43] have emerged with remarkable language understanding and reasoning abilities. Despite the above advantages, LLMs may struggle with tasks in certain specialized domains, leading to inaccurate outputs [12, 30]. Consequently, researchers leverage these powerful LLMs as tools planner [36] and intelligent agents [39], adaptively coordinating domain-specific expert models based on external demands. For example, MM-REACT [56] tackles various multimodal reasoning and action tasks via prompting ChatGPT [4] to invoke domain experts. [36, 38] embeds external API tags within text sequences to enhance LLMs’ interaction with external resources. With appropriate instruction tuning, researchers have enabled LLMs to adapt to a broader range of tasks, allowing for more specialized task planning [15, 32, 38, 41, 54]. These lines of work demonstrate that the agent is capable of receiving environmental feedback and generating optimal actions accordingly.

Recently, LLMs have garnered attention within the image processing community. For example, LM4LV [65] employs a frozen pre-trained LLM as the backbone for various image restoration tasks. Du *et al.* [10] leverage rich prior knowledge from pre-trained LLM to perform lossless image compression.

Different from these great efforts, we propose the first LLM-based agent to handle any customized optimization objectives for image processing models, named LossAgent. By leveraging the powerful understanding and reasoning capabilities of LLMs, we transform feedback from external models or metrics into appropriate adjustments of loss weights for image processing models, allowing image processing models to be *optimized* toward any objectives. We hope that our LossAgent will facilitate the development of image processing to be more open-ended and intelligent.

3. Methods

3.1. Motivation

Although the network structures of image processing models have evolved significantly in recent years, the optimization objectives of these models have remained largely unchanged. Taking image super-resolution (ISR) as an example, early works [9, 23, 64] pursued higher PSNR values, while some recent works [11, 48, 52, 58, 59, 62] have started optimizing

networks to better align with human perception considering metrics such as LPIPS [63] and NIQE [31]. Despite advances in these ISR models, image quality assessment (IQA) models have concurrently experienced significant developments. An IQA model evaluates the visual quality of images by analyzing their attributes and detecting any distortions or imperfections, making it particularly suitable as an optimization objective for image processing models [44, 55]. Given the general unavailability of reference images in practical applications, most state-of-the-art IQA metrics adopt the no-reference (NR) paradigm.

However, directly applying NR metrics as loss function for image processing model results in unstable training and suboptimal results, since they fail to effectively guide the model in capturing the structural information of images. Nevertheless, due to the specific operations in large model-based IQA metrics (*e.g.*, incorporating other models and applying sampling [50, 51, 57]), some advanced IQA metrics are non-differentiable, preventing them from being utilized as the optimization objectives during the training of image processing models. Moreover, when leveraging textual feedback from humans or MLLM-based IQA models such as Co-Instruct [51] for optimization objectives, the metrics derived from these objectives are inherently non-differentiable. Consequently, we raise a significant and interesting question “How to optimize an image processing model with these advanced IQA metrics?”

In this paper, we address the above challenges by introducing an LLM-based agent, as shown in Figure 1. Instead of directly applying these optimization objectives as loss functions for training image processing models, LossAgent efficiently transfers various forms of feedback from customized optimization objectives into an actionable weighted composition of a set of commonly used loss functions.

3.2. Weighted Compositional Loss Repository

To achieve any optimization trajectory in the training stage of image processing models, we establish the compositional loss repository with multiple typical differential loss functions $\{L_1, L_2, L_3, \dots, L_M\}$, such as L_1 and LPIPS losses, where the weighted composition of them with coefficients $\{w_1, w_2, w_3, \dots, w_M\}$ is formed to the final loss for optimizing image processing models:

$$\mathcal{L} = w_1 L_1 + w_2 L_2 + \dots + w_M L_M. \quad (1)$$

Here, M is the total number of loss functions. Based on the above weighted compositional loss repository, we can adjust the optimization direction directly by generating the weighting coefficients through our proposed loss agent. To enable the loss agent to adjust weight composition in time based on feedback from any optimization objective, we divide the training stage of the image processing model into N stages, where the current state of the image processing model and

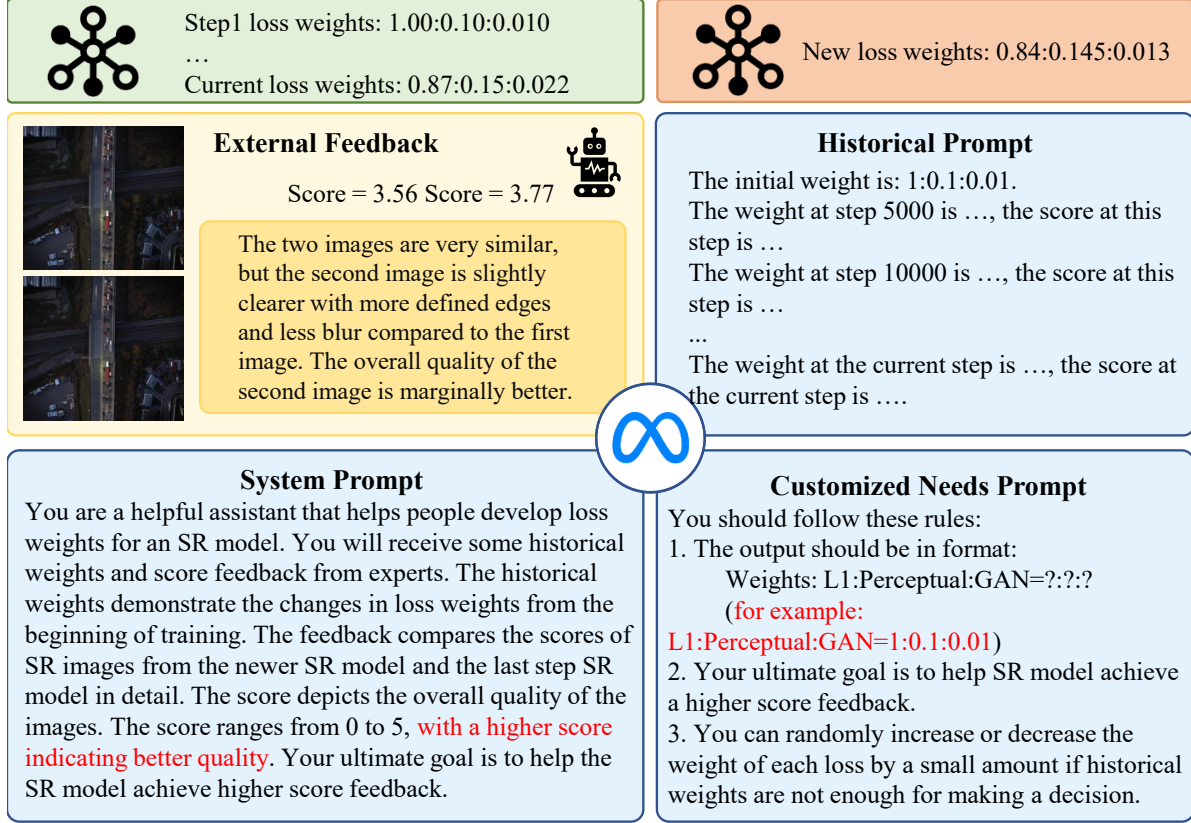


Figure 2. The overview of LossAgent. LossAgent bridges image processing models with any optimization objectives through the following workflow: The **image processing model** will generate images using weights at the current stage. Subsequently, **external expert model** will generate scores or textual feedback according to the images provided by the **image processing model**. The LLM-based **agent** model (*e.g.*, **LLaMA3**) collects feedback and leverages its powerful reasoning abilities to analyze the relationships between loss weights and optimization objectives while following our prompt engineering, including system prompt, historical prompt, and customized needs prompt. After proper analysis, the **agent** will generate a **new combination of loss weights** to further guide the next step in optimizing the **image processing model**. We provide a detailed **case study** in Section 9.

their corresponding compositional loss is as:

$$\mathcal{S} = \{S_0, S_1, S_2, \dots, S_i, \dots, S_N\}, \quad (2)$$

$$\mathcal{L}_i = w_1^i L_1 + w_2^i L_2 + \dots + w_M^i L_M, \quad (3)$$

where S_0 stands for the initial states of the image processing model and i indicates the i^{th} training stage. The external feedback will be generated by the optimization objectives at the end of each training stage with a set of randomly selected testing images as:

$$\mathcal{I} = \{I_1, I_2, \dots, I_T\}, \quad (4)$$

where T is the number of images. We provide the details for \mathcal{I} in the **Datasets** part of Section 4.1.

3.3. External Feedback

To alleviate the cognitive burden on the loss agent for the image processing task, we introduce the external evaluation expert \mathcal{O} to produce the optimization feedback to the loss

agent. Concretely, once we obtained the restored images \mathcal{I}_{S_i} at the stage S_i , we can utilize external evaluation expert \mathcal{O} to evaluate the quality of restored images \mathcal{I}_{S_i} as:

$$\mathcal{F} = \mathcal{O}(\mathcal{I}_{S_i}), \quad (5)$$

where \mathcal{F} is the external feedback from optimization objectives, which can be a quality score or textual description. Notably, the external evaluation expert is the tool to represent the optimization objective. For instance, if the optimization objective is to achieve a higher CLIPQA [44] score, we select CLIPQA as the external evaluation expert. Conversely, when the optimization objective is more general (*e.g.*, to achieve higher quality), multiple evaluation experts can be utilized collaboratively to generate feedback. We provide more details in Section 4.2.2.

3.4. Loss Agent

It is noteworthy that the current LLM cannot be directly applied to image processing tasks due to the knowledge

discrepancy. To equip the LLM with the capability to understand the image processing task and adjust the optimization direction of image processing, we further exploit prompt engineering to adapt the pre-trained LLM to our desired loss agent. Concretely, our proposed prompt engineering strategy can be divided into three parts: i) **system prompt**, ii) **historical prompt**, and iii) **customized needs prompt**.

After feedback \mathcal{F} is generated from external expert models, the loss agent will collect and utilize this feedback to update a new set of loss weights. LLM demonstrates exceptional capabilities in following instructions and making decisions [33, 38, 43]. Consequently, enabling the loss agent to accomplish our task is feasible by providing accurate and sufficient prompt guidance. Initially, we employ prompt engineering through **system prompt** approach following previous works [32, 38, 41, 54] to convey to the loss agent the role it needs to undertake, the inputs it will receive, the required outputs, and the objectives to be achieved. An example of our prompt engineering under the ISR scenario is given in Figure 2. The most important instruction for the agent is the objectives clarification: “*Your ultimate goal is to help the SR model achieve higher score feedback.*”. This is because LLM may not encompass the knowledge of how these IQA metrics should be evaluated. Therefore, it is crucial to clarify whether lower or higher scores indicate better image quality. Without this context, LLM might intuitively assume that higher scores indicate better quality, resulting in incorrect reasoning (Table 6).

Subsequently, to mitigate the hallucination phenomenon in LLM and prevent undesirable responses in situations of information scarcity, we gather the optimization trajectory of the loss agent as **historical prompt** and provide this information as context to the LLM.

Following this, we impose certain *rule-based constraints* on LLM through **customized needs prompt**. Furthermore, we incorporate format regularization into these rules to alleviate the challenge of parsing LLM outputs, which we found to be highly effective in standardizing the outputs. It is noteworthy that the design of such **customized needs prompt** not only provides flexibility for current usage but also accommodates a variety of future needs.

Ultimately, the loss agent consolidates all received information, leveraging its robust understanding and reasoning capabilities to generate a new set of loss weights as:

$$\mathcal{L}_{i+1} = w_1^{i+1}L_1 + w_2^{i+1}L_2 + \cdots + w_M^{i+1}L_M. \quad (6)$$

This new combination of loss functions will be employed to optimize the image processing model at stage $i + 1$. Based on the system prompt, the historical prompt, and the customized needs prompt, our LossAgent is capable of *updating reasonable new loss weights* for training the image processing model. Please refer to Section 4.3 for more details.

4. Experiments

4.1. Settings

To demonstrate the effectiveness of our LossAgent, we perform the evaluation on three representative low-level image processing tasks: classical image super-resolution, real-world image super-resolution, and all-in-one image restoration. We adopt two typical image processing models: SwinIR [22] for super-resolution tasks and PromptIR [34] for all-in-one restoration task. To demonstrate the effectiveness of LossAgent towards various optimization objectives, we assess the performance of our method across three testing settings: single optimization objective, double optimization objectives, and textual optimization objectives. For all score-based IQA optimization objectives, we adopt their `pyiqa` python implementation [5]. We select open-sourced Meta-Llama-3-8B-Instruct¹ as the LLM of our loss agent due to its impressive reasoning capabilities. We provide the training details in Section 6. To simplify the reasoning process of LLM, we set the number of loss functions in the loss repository to $M = 3$ in all experiments.

We mainly compare our LossAgent with three methods: i) “Pre-trained”: the official weights provided by each image processing model. ii) “Random”: the loss weights are randomly updated in each stage. iii) “Fixed”: the loss weights are fixed during the training process, the fixed values are demonstrated in Table 2.

Datasets. For image SR tasks, we follow previous works [22, 48] and adopt DF2K [1, 42] as the training dataset. For all-in-one image restoration task, we follow [19, 34] to use a combination of BSD400 [2], WED [26], Rain100L [53] and SOTS [18] to optimize the model. We utilize five SR benchmarks with ground-truth to evaluate the performance of LossAgent on classical image SR: Set5 [3], Set14 [61], BSD100 [27], Urban100 [16] and Manga109 [28]. Two real-world benchmarks without ground-truth are adopted to evaluate real-world image SR: OST300 [46] and RealSRSet [62]. We follow PromptIR [34] to use SOTS(test) [18], Rain100L(test) [53] and BSD68 [27] to evaluate the all-in-one image restoration performance. For testing images \mathcal{I} mentioned in Equation 4, we randomly sample 10 images from Set14 [61] for classical image SR; randomly sample 10 images from RealSRSet [62] for real-world image SR; randomly sample 10 images from evaluation sets of PromptIR for all-in-one IR.

4.2. Evaluation on Optimization Objectives

4.2.1. Single Optimization Objective

In this section, we validate the effectiveness of LossAgent towards the single optimization objective. We select four IQA metrics as the optimization objective: NIQE [31],

¹<https://huggingface.co/meta-llama/Meta-Llama-3-8B-Instruct>

Table 1. Quantitative comparisons between LossAgent and other methods on classical image SR. “Pre-trained” denotes the pre-trained weight. “Random” denotes that we randomly update loss weights. “Fixed” denotes that we train the model with fixed loss weights. As NIQE [31], MANIQA [55], CLIPQA [44], and Q-Align [50] are no-reference IQA metrics, we also calculate these metrics for ground-truth (GT) as a reference. \uparrow / \downarrow indicates higher/lower is better. The best results are **bolded**.

Metrics	Methods	Datasets				Avg.	
		Set5	Set14	BSD100	Urban100		
NIQE \downarrow	Pre-trained	7.10	6.22	6.11	5.46	5.37	6.05
	Random	5.12	4.16	4.07	4.08	3.99	4.28
	Fixed	5.09	4.07	3.99	4.04	3.95	4.23
	LossAgent	4.82	3.91	3.86	3.96	3.88	4.08
	GT (Ref.)	5.15	4.86	3.19	4.02	3.53	4.15
MANIQA \uparrow	Pre-trained	0.446	0.409	0.349	0.482	0.446	0.426
	Random	0.437	0.391	0.334	0.470	0.389	0.404
	Fixed	0.458	0.406	0.354	0.494	0.416	0.425
	LossAgent	0.474	0.418	0.365	0.496	0.424	0.436
	GT (Ref.)	0.534	0.449	0.523	0.552	0.420	0.496
CLIPQA \uparrow	Pre-trained	0.605	0.517	0.534	0.501	0.637	0.559
	Random	0.738	0.663	0.584	0.583	0.674	0.648
	Fixed	0.765	0.694	0.649	0.624	0.710	0.688
	LossAgent	0.788	0.718	0.679	0.643	0.729	0.711
	GT (Ref.)	0.807	0.740	0.756	0.675	0.700	0.736
Q-Align \uparrow	Pre-trained	3.03	3.29	2.98	4.38	3.65	3.47
	Random	2.99	3.32	3.15	4.40	3.65	3.50
	Fixed	3.04	3.45	3.34	4.53	3.66	3.60
	LossAgent	3.07	3.48	3.41	4.53	3.65	3.63
	GT (Ref.)	3.36	3.63	4.04	4.53	3.60	3.83

Table 2. Details of training iterations for each stage, total number of training iterations, and initial weights of loss functions for three image processing models. **For “Fixed” methods, the initial weights are fixed during the training process.**

Task	Iters. for Each Stage	Total Iters.	Initial Loss Weights
CISR	5000	100k	$\mathcal{L} = 1.0L_{L1} + 0.1L_{per} + 0.01L_{GAN}$
RISR	5000	200k	$\mathcal{L} = 1.0L_{L1} + 0.1L_{per} + 0.01L_{GAN}$
AIR	2500	100k	$\mathcal{L} = 1.0L_{L1} + 0.1L_{per} + 1.0L_{LPIPS}$

MANIQA [55], CLIPQA [44], and Q-Align [50]. For each metric, to simplify the reasoning of LLM, we start from the pre-trained weights with initial loss weights listed in Table 2, and optimize the image processing model using LossAgent with external feedback from each metric. As demonstrated in Table 1 and 3, our LossAgent outperforms “Random” and “Fixed” method (*i.e.*, fixed loss weights) across almost all the benchmarks under all the optimization objectives, which not only reveals the effectiveness of LossAgent but also indicates that our method enjoys plausible generalization abilities across different image processing models (Due to limited space, we provide results of All-in-one image restoration in Section 7). Notably, LossAgent performs well on real-world image SR task, suggesting the efficacy of our proposed method in complex application scenarios. Specifically, LossAgent outperforms the “Random” method, demonstrating that the proposed LossAgent does not update loss weights arbitrarily. On the contrary, LossAgent effectively leverages the provided prompt information to make reasonable adjustments on loss weights.

We provide qualitative comparisons between other methods and our LossAgent on classical image super-resolution tasks in Figure 3. As observed, the image processing model restores images that are more aligned with human perception with the help of LossAgent, while achieving the best IQA scores across various metrics.

4.2.2. Double Optimization Objectives

To fully explore the potential of LossAgent, we conduct an experiment on classical image SR task. In this experiment, we utilize two optimization objectives (*i.e.*, Q-Align [50] and PSNR) simultaneously to adjust loss weights. Notably, striking a balance between objective metric (*i.e.*, PSNR) and subjective metric (*i.e.*, Q-Align) is not intuitive since these two metrics are not positively correlated. However, as observed from Table 4, including PSNR as an optimization objective yields PSNR gains across all benchmarks while maintaining comparable or better Q-Align performance. We attribute this to the powerful reasoning capabilities of LLMs. Such results showcase the flexibility of LossAgent toward multiple optimization objectives.

4.2.3. Textual Optimization Objectives

While score metrics are common in image processing tasks, it is rare for tasks to utilize textual metrics as optimization objectives. Recently, Co-Instruct [51] and DepictQA [57] employed MLLMs to evaluate image quality and generate corresponding textual descriptions. To explore the flexibility and scalability of LossAgent, we choose Co-Instruct as the

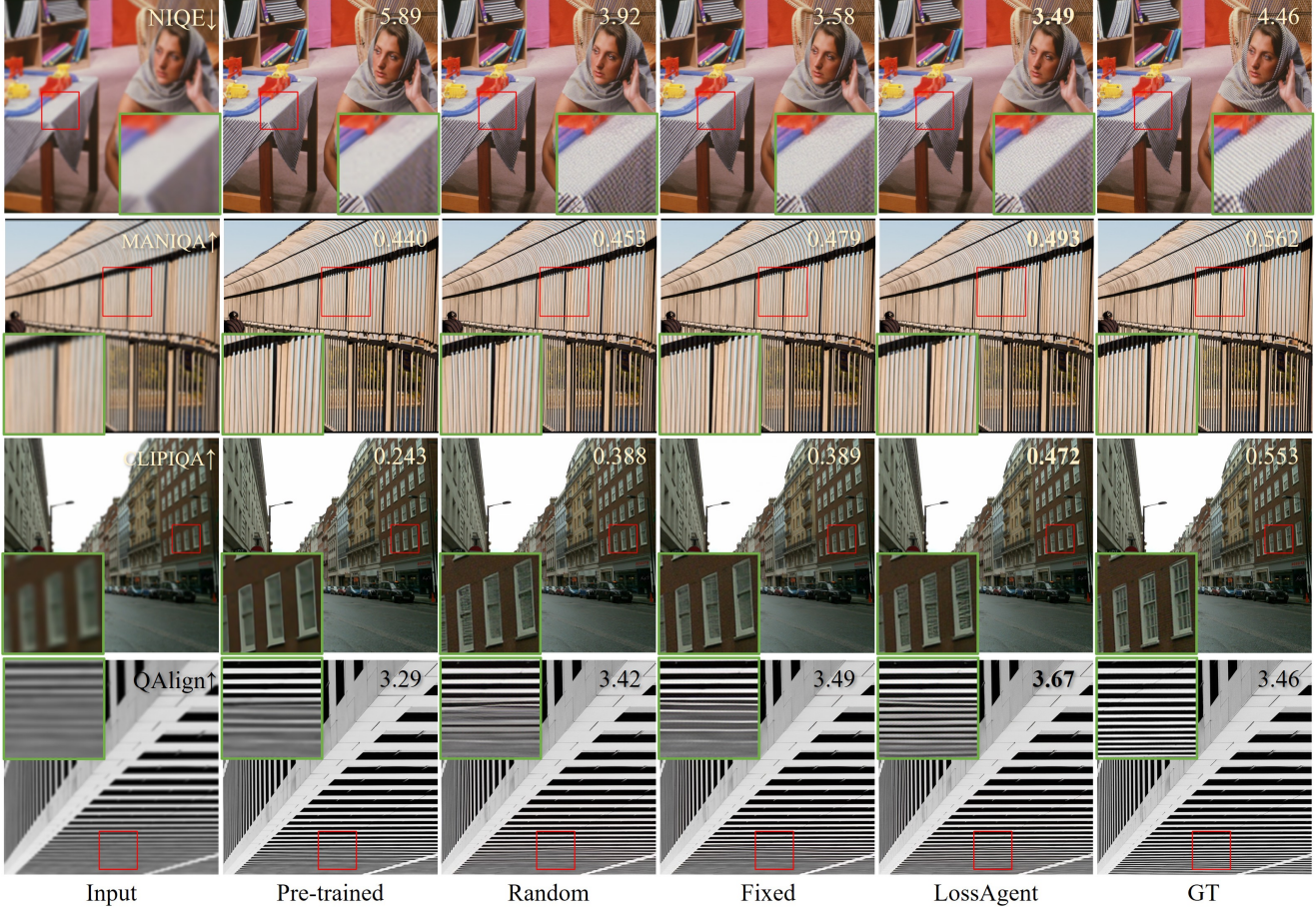


Figure 3. Qualitative comparisons between other methods and LossAgent on CISR. Zoom in for better views.

Table 3. Quantitative comparisons between LossAgent and other methods on real-world image SR. The best results are **bolded**. Notice that, there is no ground-truth for this task.

Methods	Metrics	Datasets		Avg.	Metrics	Datasets		Avg.
		OST300	RealSRSet			OST300	RealSRSet	
Pre-trained	NIQE↓	6.31	7.62	6.96	MANIQA↑	0.332	0.360	0.346
Random		4.17	5.56	4.86		0.341	0.366	0.353
Fixed		3.26	5.12	4.19		0.366	0.385	0.375
LossAgent		3.05	4.43	3.74		0.371	0.394	0.383
Pre-trained	Q-Align↑	4.47	3.43	3.95	CLIPQA↑	0.419	0.444	0.432
Random		4.39	3.73	4.06		0.357	0.407	0.382
Fixed		4.55	3.81	4.18		0.528	0.611	0.569
LossAgent		4.58	3.87	4.22		0.571	0.649	0.610

Table 4. Quantitative comparisons between single and double optimization objectives. For the latter situation, we include both Q-Align score and PSNR value as external feedback for LossAgent.

Methods	Datasets					Avg.
	Set5	Set14	BSD.	Urban.	Manga.	
Q-Align↑	3.07/30.62	3.48/27.28	3.41/26.41	4.53/25.96	3.65/29.91	3.63/28.04
Q-Align↑+PSNR↑	3.12/31.14	3.46/27.52	3.42/26.62	4.53/26.27	3.65/30.29	3.64/28.37

optimization objective. Results on all-in-one IR tasks are shown in Table 5. Notice that, there aren't any methods

available to evaluate a model optimized by textual guidance. Since Co-Instruct and Q-Align utilize similar network structures and training datasets, we find it reasonable to evaluate the performance of the Co-Instruct-optimized model by Q-Align score. As observed, the Co-Instruct-optimized model achieves comparable results with the Q-Align-optimized model, suggesting that LossAgent successfully transfers non-differentiable textual optimization objectives into appropriate adjustments of loss weights.

Summary. We have validated the flexibility and scalabil-

Table 5. Quantitative comparisons between fixed-weight model and Co-Instruct-optimized model. We use the Q-Align score to evaluate model performance.

Methods	Dehaze	Derain	Denoise			Avg.
	SOTS	Rain100L	$\sigma = 15$	$\sigma = 25$	$\sigma = 50$	
Fixed	4.03	3.94	3.95	3.94	3.76	3.92
Q-Align	3.99	3.95	3.97	3.96	3.82	3.94
Co-Instruct	4.05	3.95	3.95	3.94	3.82	3.94

ity of LossAgent in this Section through three evaluation settings: single optimization objective, double optimization objectives, and textual optimization objectives. As observed, our LossAgent is efficient towards multiple image processing tasks and various optimization objectives, which also bridges advanced IQA metrics with image processing models. Due to limited space, we provide more ablation studies about loss agent in Section 8.

4.3. Evaluation on Effectiveness of Prompt Design

As described in Section 3.4, we carefully devise prompts for the LLM to prevent hallucination and generate reasonable loss weights. Our prompt design mainly focuses on three parts: i) **System prompt** clarifies the roles and goals of LLM. Most importantly, it provides a brief introduction to these IQA metrics about whether lower or higher scores indicate better image quality. ii) **Historical prompt** accommodates previous optimization trajectories, furnishing rich context for the LLM to infer reasonable loss weights. iii) **Customized needs prompt** gives rule-based constraints on LLM’s reasoning process. Unless stated otherwise, the experiments in this section are conducted on CISR tasks.

Effectiveness of System Prompt. In Table 6, we remove the prompt that describes the relationship between scores and the qualities of images. Take NIQE [31] as an example, where a lower score indicates a better quality, LossAgent fails to improve the performance of the ISR model on the NIQE metric. We attribute this to the LLM potentially interpreting a higher score as an indicator of better quality. Consequently, our system prompt design helps mitigate hallucination in the decision-making process of LossAgent.

Table 6. Effectiveness of **system prompt**. “W/o” represents that we remove descriptions about the relationship between scores and the qualities of images from the system prompt. “W” represents system prompt with relationship-aware descriptions. We perform evaluation on CISR task with NIQE↓.

System Prompt	Datasets					Avg.
	Set5	Set14	BSD.	Urban.	Manga.	
w/o	5.12	4.24	4.02	4.17	4.06	4.32
w/	4.82	3.91	3.86	3.96	3.88	4.08

Effectiveness of Historical Prompt. Although LLM possesses strong reasoning and decision-making capabilities, it is unable to generate rational loss weights effectively with-

out sufficient context. Therefore, we provide such context by collecting all historical optimization trajectories. As demonstrated in Table 7, providing full historical information through prompt achieves the best performance, while providing only two trajectories (*i.e.*, loss weights and feedback at stage S_i and S_{i-1}) leading to performance drops.

Effectiveness of Customized Needs Prompt. As LLM generates textual outputs, it is necessary to standardize its outputs by rule-based constraints, making the weights identifiable by programs. We empirically find that given an example of the format effectively reduces hallucination in LLM’s outputs. We validate this through the correct rate of output format, as shown in Table 8. Removing this example leads to a significant drop in the successful rate of generating standardized output. In contrast, our LossAgent successfully generates standardized output, with only one failure case out of 800 samples. This demonstrates the effectiveness of our customized needs prompt design.

Table 7. Effectiveness of **historical prompt**. S_i represents the current stage, while S_0 represents the initial stage. We perform evaluation with MANIQA↑ metric.

Trajectories	Datasets					Avg.
	Set5	Set14	BSD.	Urban.	Manga.	
$\{S_{i-1}, S_i\}$	0.464	0.405	0.364	0.487	0.413	0.427
$\{S_0, \dots, S_i\}$	0.474	0.418	0.365	0.496	0.424	0.436

Table 8. Effectiveness of formatting rules. The success rate is calculated across the entire training.

Methods	Successful Rate	Methods	Successful Rate
W/o Example	21.37% (171/800)	LossAgent	99.87% (799/800)

Summary. In this Section, we have validated the effectiveness and significance of our prompt design. As demonstrated through ablations of system prompt, historical prompt and customized needs prompt, our LossAgent is capable of surpassing hallucinations and generating reasonable loss weights for image processing models.

5. Conclusion

In this paper, we propose the first loss agent to address any customized optimization objectives for low-level image processing tasks. By introducing the powerful LLM as the loss agent, our LossAgent is capable of understanding various optimization objectives, trajectories, and stage feedback from external expert models. To make the most of the reasoning abilities of LLM, we carefully design the optimization-oriented prompt engineering for the LossAgent by providing detailed instructions along with historical information to prevent hallucinations and incorrect reasoning caused by the LLM. Extensive experiments on three representative low-level image processing tasks with various customized optimization objectives have demonstrated the flexibility and scalability of LossAgent.

References

[1] Eirikur Agustsson and Radu Timofte. Ntire 2017 challenge on single image super-resolution: Dataset and study. In *Proceedings of the IEEE conference on computer vision and pattern recognition workshops*, pages 126–135, 2017. 5, 13

[2] Pablo Arbelaez, Michael Maire, Charless Fowlkes, and Jitendra Malik. Contour detection and hierarchical image segmentation. *IEEE transactions on pattern analysis and machine intelligence*, 33(5):898–916, 2010. 5

[3] Marco Bevilacqua, Aline Roumy, Christine Guillemot, and Marie Line Alberi-Morel. Low-complexity single-image super-resolution based on nonnegative neighbor embedding. 2012. 5

[4] Tom Brown, Benjamin Mann, Nick Ryder, Melanie Subbiah, Jared D Kaplan, Prafulla Dhariwal, Arvind Neelakantan, Pranav Shyam, Girish Sastry, Amanda Askell, et al. Language models are few-shot learners. *Advances in neural information processing systems*, 33:1877–1901, 2020. 1, 3

[5] Chaofeng Chen and Jiadi Mo. IQA-PyTorch: Pytorch toolbox for image quality assessment. [Online]. Available: <https://github.com/chaofengc/IQA-PyTorch>, 2022. 5

[6] Xiangyu Chen, Xintao Wang, Jiantao Zhou, Yu Qiao, and Chao Dong. Activating more pixels in image super-resolution transformer. In *Proceedings of the IEEE/CVF conference on computer vision and pattern recognition*, pages 22367–22377, 2023. 1, 2, 15

[7] Zheng Chen, Yulun Zhang, Jinjin Gu, Linghe Kong, Xiaokang Yang, and Fisher Yu. Dual aggregation transformer for image super-resolution. In *Proceedings of the IEEE/CVF international conference on computer vision*, pages 12312–12321, 2023. 1, 2

[8] Marcos V Conde, Gregor Geigle, and Radu Timofte. High-quality image restoration following human instructions. *arXiv preprint arXiv:2401.16468*, 2024. 1

[9] Chao Dong, Chen Change Loy, Kaiming He, and Xiaoou Tang. Image super-resolution using deep convolutional networks. *IEEE transactions on pattern analysis and machine intelligence*, 38(2):295–307, 2015. 2, 3

[10] Junhao Du, Chuqin Zhou, Ning Cao, Gang Chen, Yunuo Chen, Zhengxue Cheng, Li Song, Guo Lu, and Wenjun Zhang. Large language model for lossless image compression with visual prompts. *arXiv preprint arXiv:2502.16163*, 2025. 3

[11] Ben Fei, Zhaoyang Lyu, Liang Pan, Junzhe Zhang, Weidong Yang, Tianyue Luo, Bo Zhang, and Bo Dai. Generative diffusion prior for unified image restoration and enhancement. In *Proceedings of the IEEE/CVF Conference on Computer Vision and Pattern Recognition*, pages 9935–9946, 2023. 1, 2, 3

[12] Yingqiang Ge, Wenyue Hua, Kai Mei, Juntao Tan, Shuyuan Xu, Zelong Li, Yongfeng Zhang, et al. Openagi: When llm meets domain experts. *Advances in Neural Information Processing Systems*, 36, 2024. 1, 3

[13] Hang Guo, Yong Guo, Yaohua Zha, Yulun Zhang, Wenbo Li, Tao Dai, Shu-Tao Xia, and Yawei Li. Mambairv2: Attentive state space restoration. *arXiv preprint arXiv:2411.15269*, 2024. 15

[14] Hang Guo, Jinmin Li, Tao Dai, Zhihao Ouyang, Xudong Ren, and Shu-Tao Xia. Mambair: A simple baseline for image restoration with state-space model. In *European conference on computer vision*, pages 222–241. Springer, 2024. 15

[15] Tanmay Gupta and Aniruddha Kembhavi. Visual programming: Compositional visual reasoning without training. In *Proceedings of the IEEE/CVF Conference on Computer Vision and Pattern Recognition*, pages 14953–14962, 2023. 1, 3

[16] Jia-Bin Huang, Abhishek Singh, and Narendra Ahuja. Single image super-resolution from transformed self-exemplars. In *Proceedings of the IEEE conference on computer vision and pattern recognition*, pages 5197–5206, 2015. 5

[17] Christian Ledig, Lucas Theis, Ferenc Huszár, Jose Caballero, Andrew Cunningham, Alejandro Acosta, Andrew Aitken, Alykhan Tejani, Johannes Totz, Zehan Wang, et al. Photo-realistic single image super-resolution using a generative adversarial network. In *Proceedings of the IEEE conference on computer vision and pattern recognition*, pages 4681–4690, 2017. 1, 2

[18] Boyi Li, Wenqi Ren, Dengpan Fu, Dacheng Tao, Dan Feng, Wenjun Zeng, and Zhangyang Wang. Benchmarking single-image dehazing and beyond. *IEEE Transactions on Image Processing*, 28(1):492–505, 2018. 5

[19] Boyun Li, Xiao Liu, Peng Hu, Zhongqin Wu, Jiancheng Lv, and Xi Peng. All-in-one image restoration for unknown corruption. In *Proceedings of the IEEE/CVF Conference on Computer Vision and Pattern Recognition*, pages 17452–17462, 2022. 5

[20] Junnan Li, Dongxu Li, Silvio Savarese, and Steven Hoi. Blip-2: Bootstrapping language-image pre-training with frozen image encoders and large language models. In *International conference on machine learning*, pages 19730–19742. PMLR, 2023. 3

[21] Yawei Li, Yuchen Fan, Xiaoyu Xiang, Denis Demandolx, Rakesh Ranjan, Radu Timofte, and Luc Van Gool. Efficient and explicit modelling of image hierarchies for image restoration. In *Proceedings of the IEEE/CVF Conference on Computer Vision and Pattern Recognition*, pages 18278–18289, 2023. 1

[22] Jingyun Liang, Jiezhang Cao, Guolei Sun, Kai Zhang, Luc Van Gool, and Radu Timofte. Swinir: Image restoration using swin transformer. In *Proceedings of the IEEE/CVF international conference on computer vision*, pages 1833–1844, 2021. 1, 2, 5, 12

[23] Bee Lim, Sanghyun Son, Heewon Kim, Seungjun Nah, and Kyoung Mu Lee. Enhanced deep residual networks for single image super-resolution. In *Proceedings of the IEEE conference on computer vision and pattern recognition workshops*, pages 136–144, 2017. 2, 3

[24] Pan Lu, Baolin Peng, Hao Cheng, Michel Galley, Kai-Wei Chang, Ying Nian Wu, Song-Chun Zhu, and Jianfeng Gao. Chameleon: Plug-and-play compositional reasoning with large language models. *Advances in Neural Information Processing Systems*, 36, 2024. 1

[25] Jiaqi Ma, Tianheng Cheng, Guoli Wang, Qian Zhang, Xinggang Wang, and Lefei Zhang. Prores: Exploring degradation-

aware visual prompt for universal image restoration. *arXiv preprint arXiv:2306.13653*, 2023. 2

[26] Kede Ma, Zhengfang Duanmu, Qingbo Wu, Zhou Wang, Hongwei Yong, Hongliang Li, and Lei Zhang. Waterloo exploration database: New challenges for image quality assessment models. *IEEE Transactions on Image Processing*, 26(2):1004–1016, 2016. 5

[27] David Martin, Charless Fowlkes, Doron Tal, and Jitendra Malik. A database of human segmented natural images and its application to evaluating segmentation algorithms and measuring ecological statistics. In *Proceedings Eighth IEEE International Conference on Computer Vision. ICCV 2001*, pages 416–423. IEEE, 2001. 5

[28] Yusuke Matsui, Kota Ito, Yuji Aramaki, Azuma Fujimoto, Toru Ogawa, Toshihiko Yamasaki, and Kiyoharu Aizawa. Sketch-based manga retrieval using manga109 dataset. *Multimedia Tools and Applications*, 76(20):21811–21838, 2017. 5

[29] MetaAI. Llama3. <https://llama.meta.com/llama3>, 2024. 1

[30] Grégoire Mialon, Roberto Dessì, Maria Lomeli, Christoforos Nalpantis, Ram Pasunuru, Roberta Raileanu, Baptiste Rozière, Timo Schick, Jane Dwivedi-Yu, Asli Celikyilmaz, et al. Augmented language models: a survey. *arXiv preprint arXiv:2302.07842*, 2023. 3

[31] Anish Mittal, Rajiv Soundararajan, and Alan C Bovik. Making a “completely blind” image quality analyzer. *IEEE Signal processing letters*, 20(3):209–212, 2012. 3, 5, 6, 8, 12

[32] Yao Mu, Qinglong Zhang, Mengkang Hu, Wenhui Wang, Mingyu Ding, Jun Jin, Bin Wang, Jifeng Dai, Yu Qiao, and Ping Luo. Embodiedgpt: Vision-language pre-training via embodied chain of thought. *Advances in Neural Information Processing Systems*, 36, 2024. 1, 3, 5

[33] OpenAI. Gpt-4 technical report, 2023. 1, 5

[34] Vaishnav Potlapalli, Syed Waqas Zamir, Salman Khan, and Fahad Shahbaz Khan. Promptir: Prompting for all-in-one blind image restoration. *arXiv preprint arXiv:2306.13090*, 2023. 2, 5, 12

[35] Baptiste Rozière, Jonas Gehring, Fabian Gloeckle, Sten Sootla, Itai Gat, Xiaoqing Ellen Tan, Yossi Adi, Jingyu Liu, Tal Remez, Jérémie Rapin, et al. Code llama: Open foundation models for code. *arXiv preprint arXiv:2308.12950*, 2023. 1

[36] Timo Schick, Jane Dwivedi-Yu, Roberto Dessì, Roberta Raileanu, Maria Lomeli, Eric Hambro, Luke Zettlemoyer, Nicola Cancedda, and Thomas Scialom. Toolformer: Language models can teach themselves to use tools. *Advances in Neural Information Processing Systems*, 36, 2024. 1, 3

[37] Raphael Schumann, Wanrong Zhu, Weixi Feng, Tsu-Jui Fu, Stefan Riezler, and William Yang Wang. Velma: Verbalization embodiment of llm agents for vision and language navigation in street view. In *Proceedings of the AAAI Conference on Artificial Intelligence*, pages 18924–18933, 2024. 1

[38] Yongliang Shen, Kaitao Song, Xu Tan, Dongsheng Li, Weiming Lu, and Yuetong Zhuang. Hugginggpt: Solving ai tasks with chatgpt and its friends in hugging face. *Advances in Neural Information Processing Systems*, 36, 2024. 1, 3, 5

[39] Noah Shinn, Federico Cassano, Ashwin Gopinath, Karthik Narasimhan, and Shunyu Yao. Reflexion: Language agents with verbal reinforcement learning. *Advances in Neural Information Processing Systems*, 36, 2024. 1, 3

[40] Karen Simonyan and Andrew Zisserman. Very deep convolutional networks for large-scale image recognition. *arXiv preprint arXiv:1409.1556*, 2014. 2

[41] Dídac Surís, Sachit Menon, and Carl Vondrick. Vipergpt: Visual inference via python execution for reasoning. In *Proceedings of the IEEE/CVF International Conference on Computer Vision*, pages 11888–11898, 2023. 1, 3, 5

[42] Radu Timofte, Eirikur Agustsson, Luc Van Gool, Ming-Hsuan Yang, and Lei Zhang. Ntire 2017 challenge on single image super-resolution: Methods and results. In *Proceedings of the IEEE conference on computer vision and pattern recognition workshops*, pages 114–125, 2017. 5

[43] Hugo Touvron, Louis Martin, Kevin Stone, Peter Albert, Amjad Almahairi, Yasmine Babaci, Nikolay Bashlykov, Soumya Batra, Prajjwal Bhargava, Shruti Bhosale, et al. Llama 2: Open foundation and fine-tuned chat models. *arXiv preprint arXiv:2307.09288*, 2023. 1, 3, 5

[44] Jianyi Wang, Kelvin CK Chan, and Chen Change Loy. Exploring clip for assessing the look and feel of images. In *Proceedings of the AAAI Conference on Artificial Intelligence*, pages 2555–2563, 2023. 3, 4, 6, 12

[45] Tao Wang, Kaihao Zhang, Tianrun Shen, Wenhan Luo, Bjorn Stenger, and Tong Lu. Ultra-high-definition low-light image enhancement: A benchmark and transformer-based method. In *Proceedings of the AAAI Conference on Artificial Intelligence*, pages 2654–2662, 2023. 2

[46] Xintao Wang, Ke Yu, Chao Dong, and Chen Change Loy. Recovering realistic texture in image super-resolution by deep spatial feature transform. In *Proceedings of the IEEE conference on computer vision and pattern recognition*, pages 606–615, 2018. 1, 5

[47] Xintao Wang, Ke Yu, Shixiang Wu, Jinjin Gu, Yihao Liu, Chao Dong, Yu Qiao, and Chen Change Loy. Esrgan: Enhanced super-resolution generative adversarial networks. In *Proceedings of the European conference on computer vision (ECCV) workshops*, pages 0–0, 2018. 2

[48] Xintao Wang, Liangbin Xie, Chao Dong, and Ying Shan. Real-esrgan: Training real-world blind super-resolution with pure synthetic data. In *Proceedings of the IEEE/CVF international conference on computer vision*, pages 1905–1914, 2021. 1, 2, 3, 5

[49] Xinlong Wang, Wen Wang, Yue Cao, Chunhua Shen, and Tiejun Huang. Images speak in images: A generalist painter for in-context visual learning. In *Proceedings of the IEEE/CVF Conference on Computer Vision and Pattern Recognition*, pages 6830–6839, 2023. 2

[50] Haoning Wu, Zicheng Zhang, Weixia Zhang, Chaofeng Chen, Liang Liao, Chunyi Li, Yixuan Gao, Annan Wang, Erli Zhang, Wenxiu Sun, et al. Q-align: Teaching lmms for visual scoring via discrete text-defined levels. *arXiv preprint arXiv:2312.17090*, 2023. 2, 3, 6

[51] Haoning Wu, Hanwei Zhu, Zicheng Zhang, Erli Zhang, Chaofeng Chen, Liang Liao, Chunyi Li, Annan Wang,

Wenxiu Sun, Qiong Yan, Xiaohong Liu, Guangtao Zhai, Shiqi Wang, and Weisi Lin. Towards open-ended visual quality comparison, 2024. [2](#), [3](#), [6](#)

[52] Bin Xia, Yulun Zhang, Shiyin Wang, Yitong Wang, Xinglong Wu, Yapeng Tian, Wenming Yang, and Luc Van Gool. Diffir: Efficient diffusion model for image restoration. In *Proceedings of the IEEE/CVF International Conference on Computer Vision*, pages 13095–13105, 2023. [1](#), [2](#), [3](#)

[53] Fuzhi Yang, Huan Yang, Jianlong Fu, Hongtao Lu, and Baineng Guo. Learning texture transformer network for image super-resolution. In *Proceedings of the IEEE/CVF conference on computer vision and pattern recognition*, pages 5791–5800, 2020. [5](#)

[54] Jingkang Yang, Yuhao Dong, Shuai Liu, Bo Li, Ziyue Wang, Chencheng Jiang, Haoran Tan, Jiamu Kang, Yuanhan Zhang, Kaiyang Zhou, et al. Octopus: Embodied vision-language programmer from environmental feedback. *arXiv preprint arXiv:2310.08588*, 2023. [1](#), [3](#), [5](#)

[55] Sidi Yang, Tianhe Wu, Shuwei Shi, Shanshan Lao, Yuan Gong, Mingdeng Cao, Jiahao Wang, and Yujiu Yang. Maniq: Multi-dimension attention network for no-reference image quality assessment. In *Proceedings of the IEEE/CVF Conference on Computer Vision and Pattern Recognition*, pages 1191–1200, 2022. [3](#), [6](#)

[56] Zhengyuan Yang, Linjie Li, Jianfeng Wang, Kevin Lin, Ehsan Azarnasab, Faisal Ahmed, Zicheng Liu, Ce Liu, Michael Zeng, and Lijuan Wang. Mm-react: Prompting chatgpt for multimodal reasoning and action. *arXiv preprint arXiv:2303.11381*, 2023. [1](#), [3](#)

[57] Zhiyuan You, Zheyuan Li, Jinjin Gu, Zhenfei Yin, Tianfan Xue, and Chao Dong. Depicting beyond scores: Advancing image quality assessment through multi-modal language models. In *European Conference on Computer Vision*, pages 259–276. Springer, 2024. [2](#), [3](#), [6](#)

[58] Fanghua Yu, Jinjin Gu, Zheyuan Li, Jinfan Hu, Xiangtao Kong, Xintao Wang, Jingwen He, Yu Qiao, and Chao Dong. Scaling up to excellence: Practicing model scaling for photo-realistic image restoration in the wild. *arXiv preprint arXiv:2401.13627*, 2024. [1](#), [2](#), [3](#)

[59] Zongsheng Yue, Jianyi Wang, and Chen Change Loy. Resshift: Efficient diffusion model for image super-resolution by residual shifting. *Advances in Neural Information Processing Systems*, 36, 2024. [1](#), [2](#), [3](#)

[60] Syed Waqas Zamir, Aditya Arora, Salman Khan, Munawar Hayat, Fahad Shahbaz Khan, and Ming-Hsuan Yang. Restormer: Efficient transformer for high-resolution image restoration. In *Proceedings of the IEEE/CVF conference on computer vision and pattern recognition*, pages 5728–5739, 2022. [1](#)

[61] Roman Zeyde, Michael Elad, and Matan Protter. On single image scale-up using sparse-representations. In *International conference on curves and surfaces*, pages 711–730. Springer, 2010. [5](#), [13](#)

[62] Kai Zhang, Jingyun Liang, Luc Van Gool, and Radu Timofte. Designing a practical degradation model for deep blind image super-resolution. In *Proceedings of the IEEE/CVF International Conference on Computer Vision*, pages 4791–4800, 2021. [1](#), [2](#), [3](#), [5](#)

[63] Richard Zhang, Phillip Isola, Alexei A Efros, Eli Shechtman, and Oliver Wang. The unreasonable effectiveness of deep features as a perceptual metric. In *Proceedings of the IEEE conference on computer vision and pattern recognition*, pages 586–595, 2018. [3](#)

[64] Yulun Zhang, Yapeng Tian, Yu Kong, Bineng Zhong, and Yun Fu. Residual dense network for image super-resolution. In *Proceedings of the IEEE conference on computer vision and pattern recognition*, pages 2472–2481, 2018. [2](#), [3](#)

[65] Boyang Zheng, Jinjin Gu, Shijun Li, and Chao Dong. Lm4lv: A frozen large language model for low-level vision tasks. *arXiv preprint arXiv:2405.15734*, 2024. [3](#)

LossAgent: Towards Any Optimization Objectives for Image Processing with LLM Agents

Supplementary Material

6. Training Details

As demonstrated in Section 3.2, we divide the whole training process of image processing models into several stages to enable the dynamic adjustment of loss weights through LossAgent. We list the details of training iterations for each stage, the total number of training iterations, and the initial weights of loss functions in Table 2. For two image super-resolution tasks, we utilize the PSNR-oriented pre-trained weights of SwinIR [22] as initial model weights for both tasks and then apply popular losses from GAN-based training strategies for image SR tasks using our LossAgent. For all-in-one image restoration tasks, we adopt the pre-trained weight of PromptIR [34] as the initial model weight. However, since GAN-based training is uncommon for this task, we use a combination of L1 loss, perceptual loss, and LPIPS loss as the loss repository to evaluate the performance of our LossAgent. The rationale behind utilizing pre-trained weights as initial model weights is to mitigate unstable fluctuations in the early stages of training of image processing models. Such fluctuations may otherwise misguide the LossAgent due to the limited capabilities of current LLMs, leading to inaccurate updates of loss weights. It is noteworthy that, to avoid the effect from the learning rate of the optimizer on our experiments, we uniformly set the learning rate to 1e-4 for all three tasks and kept it constant throughout the training process. Following previous implementations, we utilize an Adam optimizer for each task. We use 8 NVIDIA TESLA V100 GPUs for our experiments, with a total batch-size of 32 for image SR tasks and a total batchsize of 16 for all-in-one image restoration tasks.

7. Additional Results for All-in-One Image Restoration

We provide the quantitative results of LossAgent compared to other methods on all-in-one image restoration tasks across four optimization objectives in Table 9. As demonstrated in the Table, in the all-in-one IR task, LossAgent does not perform as robustly as in the other two tasks. We attribute this to the minimal differences between images generated in consecutive stages, which limit the instructional information available to the agent from feedback and hinder its ability to conduct thorough analysis and inference to adjust loss weights. However, LossAgent still shows commendable performance improvement against other methods, indicating the flexibility and adaptability of our LossAgent across different image process models.

8. More Ablation Studies

In this section, we provide more ablation studies to verify the reliability of our design for LossAgent.

8.1. Iterations for Each Stage

In this part, we conduct ablation studies about training iterations for each stage. As demonstrated in Table 10, a moderate choice of 5000 training iterations for each stage achieves the best results. If the iterations are small (i.e., 2500), when reaching the end of training, the list of historical loss weights tends to become very long, thus making it difficult to perform reasoning. If the iterations are large (i.e., 10000), the total update steps tend to be insufficient for a reasonable adjustment of loss weights during training, thereby causing suboptimal results. Therefore, we select the optimal iteration steps for the classical image SR task to be 5000. We apply the same principle to the other two tasks, as listed in Table 2.

8.2. Objective as Loss Function vs. LossAgent

In the loss repository of LossAgent, we adopt commonly used reference-based loss functions for different tasks, such as L1 loss, LPIPS loss, and perceptual loss. LossAgent achieves the various optimization goals by adjusting the weights of these stable loss functions. However, as mentioned in Section 3.1, some advanced no-reference (NR) IQA metrics can be applied as the loss function, such as CLIPQA [44]/NIQE [31]. The primary reason for not using these metrics as loss functions in image processing model training is that such NR loss functions may lead to instability during the training process. To further validate this, we choose the CLIPQA/NIQE as the optimization objective, and compare the performance of LossAgent against directly adding CLIPQA/NIQE loss into the training process in Table 11.

It is noteworthy that, we combine three loss functions mentioned in the main paper with CLIPQA/NIQE loss instead of only utilizing CLIPQA/NIQE to optimize the model, since CLIPQA/NIQE cannot provide direct guidance on the structural restoration on images, leading to training collapse. As demonstrated in Table 11, directly adding these NR objectives as loss functions into the training process results in suboptimal performance. On the contrary, LossAgent achieves these optimization goals by leveraging the combination of existing stable loss functions.

Table 9. Quantitative comparisons between LossAgent and other methods on all-in-one IR. The best results are **bolded**.

Metrics	Methods	Dehaze		Derain			Avg.
		SOTS	Rain100L	$\sigma = 15$	$\sigma = 25$	$\sigma = 50$	
NIQE \downarrow	Pre-trained	2.91	3.16	3.77	3.96	4.25	3.61
	Fixed	2.98	3.18	3.43	3.61	3.88	3.42
	LossAgent	2.95	3.17	3.38	3.48	3.80	3.36
	GT (Ref.)	2.94	3.17	3.13	3.13	3.13	3.10
MANIQA \uparrow	Pre-trained	0.441	0.498	0.493	0.457	0.377	0.453
	Fixed	0.447	0.503	0.482	0.450	0.381	0.453
	LossAgent	0.450	0.505	0.491	0.462	0.386	0.459
	GT (Ref.)	0.442	0.509	0.525	0.525	0.525	0.505
CLIPQA \uparrow	Pre-trained	0.494	0.750	0.686	0.672	0.640	0.649
	Fixed	0.534	0.769	0.795	0.785	0.725	0.722
	LossAgent	0.542	0.771	0.807	0.777	0.706	0.721
	GT (Ref.)	0.544	0.755	0.757	0.757	0.757	0.714
Q-Align \uparrow	Pre-trained	4.02	3.92	4.09	3.96	3.61	3.92
	Fixed	4.03	3.94	3.95	3.94	3.76	3.92
	LossAgent	3.99	3.95	3.97	3.96	3.82	3.94
	GT (Ref.)	3.96	4.01	4.11	4.11	4.11	4.08

Table 10. Quantitative comparisons between different iterations for each stage. Results are reported on classical image SR (CISR) using Q-Align score. The best results are **bolded**.

Iters.	Datasets					Avg.
	Set5	Set14	BSD100	Urban100	Manga109	
2500	3.06	3.47	3.36	4.52	3.65	3.61
5000	3.07	3.48	3.41	4.53	3.65	3.63
10000	3.02	3.45	3.35	4.49	3.65	3.59

Table 11. Quantitative comparisons between directly adding optimization objective (CLIPQA/NIQE) into training process and LossAgent. Results are reported on real-world image SR (RISR). Notably, adopting CLIPQA/NIQE themselves as the only loss function results in training collapse, and we do not report these results in the table.

	Add CLIPQA \uparrow	LossAgent		Add NIQE \downarrow	LossAgent
OST300	0.202	0.571		6.59	3.05
RealSRSet	0.226	0.649		7.83	4.43

8.3. M in Loss Repository

To simplify the reasoning process of the LLM agent, we adopt the commonly-used three loss functions (*i.e.*, $M = 3$) in existing IR methods, as demonstrated in Section 4.1. However, the design of the loss repository enables LossAgent to support more loss functions. To validate this, we expand the M to five (L1, MSE, Perceptual, GAN, LPIPS) in Table 12, which demonstrates that a larger loss repository achieves slightly better results. We attribute this to the limited reason-

ing ability of the current LLM. Nevertheless, the improved results still indicate the potential of scalability of LossAgent.

8.4. Testing Image Set

As a crucial part of generating feedback from external expert models, the choice of the testing image set \mathcal{I} is important. We observe that using the sampled Set14 [61] as the testing image set achieves a better CLIPQA score compared to using the sampled DIV2K [1]. We attribute this to the relatively high resolution of the DIV2K images. Since some advanced IQA metrics leverage a pre-trained vision encoder to resize input images, this results in originally similar high-resolution images becoming even harder to distinguish after resizing. Consequently, the IQA model may assign similar or even identical scores to these images, failing to provide useful information to our LossAgent. This can cause the LLM to hallucinate and make unreasonable inferences, leading to incorrect adjustment of loss weights. As a result, we choose Set14 as the testing image set for the classical image SR task. We apply the same principle to the other two tasks.

8.5. The Illustration of Loss Weight Curves

To provide a more intuitive understanding of how LossAgent updates the loss weights, we provide a visualization of the loss weight curves on the classical image super-resolution (CISR) task in Figure 5. Notably, since the four NR objectives in the Figure are all designed for human perception, the curves theoretically exhibit similar trends at a coarse granularity, while their fine-grained preferences differ. Consequently, our LossAgent adjusts loss weights following the theoretical rules while adapting to different optimization

Table 12. Quantitative comparisons between different loss repositories for LossAgent on classical image SR. \uparrow / \downarrow indicates higher/lower is better. The best results are **bolded**.

Metrics	Methods	Datasets					Avg.
		Set5	Set14	BSD100	Urban100	Manga109	
NIQE \downarrow	LossAgent ($M = 3$)	4.82	3.91	3.86	3.96	3.88	4.08
	LossAgent ($M = 5$)	4.73	3.85	3.93	3.92	3.77	4.04
MANIQA \uparrow	LossAgent ($M = 3$)	0.474	0.418	0.365	0.496	0.424	0.436
	LossAgent ($M = 5$)	0.478	0.423	0.376	0.509	0.422	0.442
CLIPQA \uparrow	LossAgent ($M = 3$)	0.788	0.718	0.679	0.643	0.729	0.711
	LossAgent ($M = 5$)	0.768	0.711	0.684	0.634	0.723	0.704
Q-Align \uparrow	LossAgent ($M = 3$)	3.07	3.48	3.41	4.53	3.65	3.63
	LossAgent ($M = 5$)	3.14	3.52	3.48	4.52	3.64	3.66

Table 13. Quantitative comparisons between different iterations for each stage. Results are reported on classical image SR task using Q-Align score. The best results are **bolded**.

Image Set	Datasets					Avg.
	Set5	Set14	BSD100	Urban100	Manga109	
Set14	0.788	0.718	0.679	0.643	0.729	0.711
DIV2K	0.783	0.706	0.675	0.638	0.721	0.704

Table 14. Training time analysis of LossAgent on three low-level image processing tasks. “Model Training” denotes the necessary training time required by image processing models, which also serves as the reference time for LossAgent comparisons.

Task	Each Stage			Total
	Model Training	LLM Reasoning	Feedback	
CISR	566min	58min	3min	627min $\uparrow 10.78\%$
RISR	1176min	192min	20min	1388min $\uparrow 18.03\%$
AIR	516min	83min	5min	604min $\uparrow 17.05\%$

objectives.

8.6. Flexibility of LossAgent across Different Image Processing Models

In this section, we demonstrate the flexibility of LossAgent by applying two recent image restoration backbones as the image processing model. As demonstrated in Table 15 and 16, HAT-S and MambaIRv2-light optimized by LossAgent outperform other methods on almost all benchmarks across four metrics. This further demonstrates the flexibility of LossAgent toward different backbones of image processing models, indicating the great potential of LossAgent.

8.7. Time Analysis

In this section, we provide the training time analysis of LossAgent in Table 14. As demonstrated, LossAgent introduces approximately 15% extra training time averaged on three

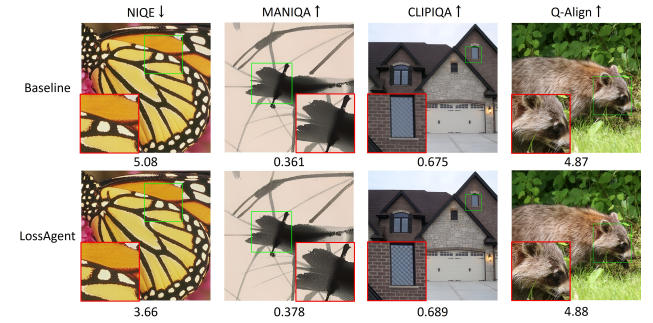


Figure 4. Qualitative comparisons between baseline and LossAgent on real-world image super-resolution across four optimization objectives. Zoom in for the best views.

training tasks. Compared to the performance improvement brought by LossAgent, we consider the additional training time to be acceptable. Notably, there is no additional time overhead during testing since we only introduce LossAgent during training.

8.8. More Qualitative Results

We provide additional qualitative comparisons between LossAgent and other methods on the real-world image super-resolution (RISR) task in Figure 4. As illustrated, the SR model optimized by LossAgent restores more vivid textures that align with optimization objectives.

9. Case Study

In this section, we provide a case study on classical image super-resolution in Figure 6 to help readers better understand the process of LossAgent. As demonstrated, LossAgent is capable of analyzing the relationships between loss weights and score feedback from the historical prompt (we mark such analysis in green). Moreover, LossAgent updates new loss weights considering not only these relationships but also the

Table 15. Quantitative comparisons between LossAgent and other methods on classical image SR based on **HAT-S** [6] backbone. \uparrow / \downarrow indicates higher/lower is better. The best results are **bolded**.

Metrics	Methods	Datasets					Avg.
		Set5	Set14	BSD100	Urban100	Manga109	
NIQE \downarrow	Pre-trained	7.06	6.29	6.05	5.45	5.21	6.01
	Fixed	4.90	4.10	3.82	4.16	4.09	4.21
	LossAgent	4.42	4.18	3.91	4.06	3.89	4.09
	GT (Ref.)	5.15	4.86	3.19	4.02	3.53	4.15
MANIQA \uparrow	Pre-trained	0.447	0.405	0.347	0.480	0.440	0.424
	Fixed	0.438	0.387	0.360	0.476	0.403	0.412
	LossAgent	0.460	0.404	0.374	0.505	0.424	0.434
	GT (Ref.)	0.534	0.449	0.523	0.552	0.420	0.496
CLIPQA \uparrow	Pre-trained	0.620	0.512	0.536	0.500	0.637	0.561
	Fixed	0.765	0.674	0.679	0.613	0.706	0.688
	LossAgent	0.740	0.711	0.681	0.636	0.728	0.699
	GT (Ref.)	0.807	0.740	0.756	0.675	0.700	0.736
Q-Align \uparrow	Pre-trained	3.03	3.29	2.95	4.37	3.65	3.46
	Fixed	2.95	3.38	3.40	4.52	3.66	3.58
	LossAgent	2.98	3.49	3.44	4.55	3.65	3.62
	GT (Ref.)	3.36	3.63	4.04	4.53	3.60	3.83

Table 16. Quantitative comparisons between LossAgent and other methods on classical image SR based on **MambaIRv2-light** [13, 14] backbone. \uparrow / \downarrow indicates higher/lower is better. The best results are **bolded**.

Metrics	Methods	Datasets					Avg.
		Set5	Set14	BSD100	Urban100	Manga109	
NIQE \downarrow	Pre-trained	6.78	6.22	6.21	5.49	5.14	5.97
	Fixed	4.95	4.10	3.85	4.08	3.84	4.17
	LossAgent	4.42	4.03	3.78	4.04	3.72	4.00
	GT (Ref.)	5.15	4.86	3.19	4.02	3.53	4.15
MANIQA \uparrow	Pre-trained	0.428	0.379	0.324	0.454	0.432	0.403
	Fixed	0.415	0.381	0.333	0.470	0.410	0.402
	LossAgent	0.435	0.395	0.348	0.464	0.436	0.415
	GT (Ref.)	0.534	0.449	0.523	0.552	0.420	0.496
CLIPQA \uparrow	Pre-trained	0.601	0.498	0.504	0.484	0.620	0.541
	Fixed	0.749	0.689	0.668	0.619	0.711	0.687
	LossAgent	0.756	0.680	0.673	0.623	0.726	0.692
	GT (Ref.)	0.807	0.740	0.756	0.675	0.700	0.736
Q-Align \uparrow	Pre-trained	2.92	3.18	2.80	4.29	3.63	3.37
	Fixed	2.82	3.33	3.25	4.52	3.61	3.50
	LossAgent	2.91	3.48	3.34	4.61	3.65	3.60
	GT (Ref.)	3.36	3.63	4.04	4.53	3.60	3.83

functionality of each loss function (we mark such thoughts in red). To get the updated loss weights, we use a python program to parse the pattern “L1:Perceptual:GAN=0.7:0.3:0.05” into the numeric array “[0.7, 0.3, 0.05]”. Therefore, the correctness of this pattern is important. As analysed in Section 4.3, we use rule-based formatting constraints, which are helpful for the LLaMA3 model.

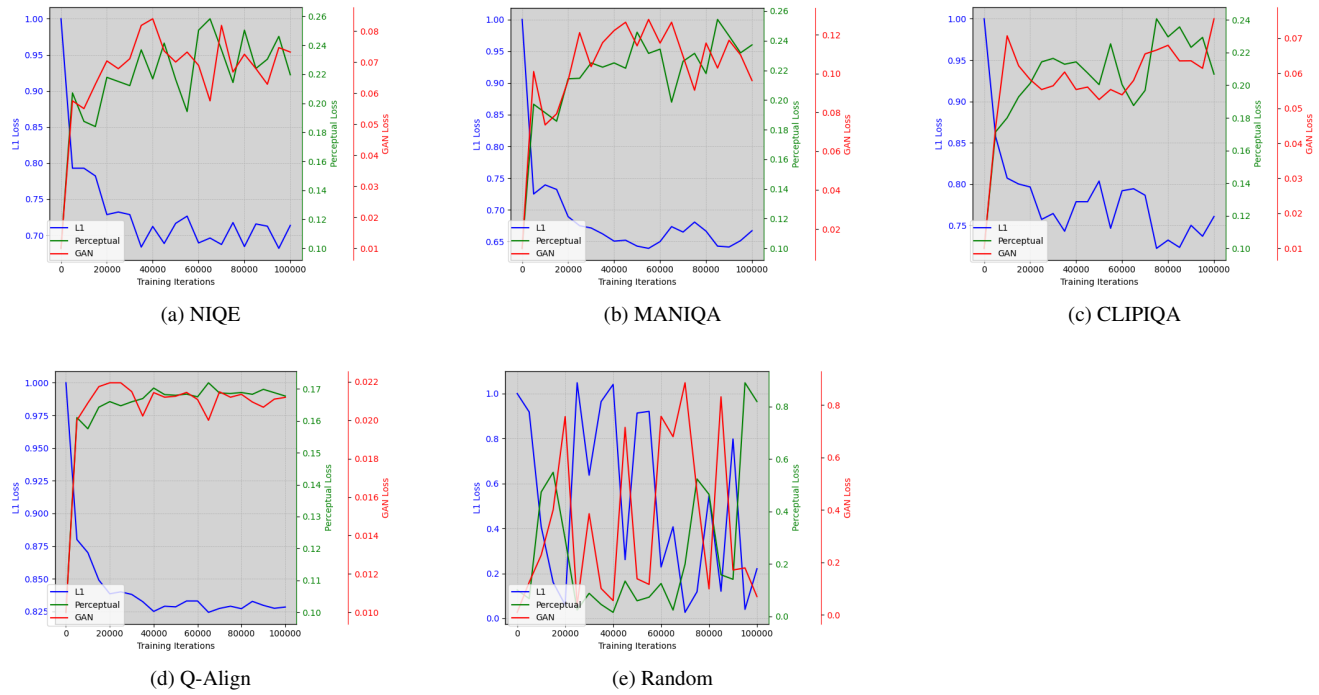


Figure 5. Illustration of loss weight curves on classical image super-resolution task across four optimization objectives. Zoom in for better views.

Case Study – NIQE, 25000 iters., Response of one sampled image from Set14

System Prompt

You are a helpful assistant that help people develop loss weights of an SR model. You will receive some historical weights, and score feedback from experts. The SR model is trained with each historical weight for fixed steps of parameter updates sequentially. The historical weights demonstrated the loss weight changes **from the beginning of training**. The feedback includes the score changes of SR images from the beginning of training in detail. The score depicts the overall quality of images. The **lower** score stands for better quality. Your ultimate goal is to help the SR model achieve a **lower** score feedback.

Historical Prompt

Feedback: Initial loss weights of L1 loss, Perceptual loss and GAN loss is 1.0:0.1:0.01. The initial score of the image before training is 4.7087. The score of the image at this step is 2.9642.

Step 5000 weights is 0.79286:0.20714:0.0575. The score of the image at this step is 2.5495

Step 10000 weights is 0.79286:0.1875:0.055. The score of the image at this step is 2.7706

Step 15000 weights is 0.78214:0.18393:0.06286. The score of the image at this step is 2.8586

Step 20000 weights is 0.72857:0.21786:0.07036. The score of the image at this step is 2.705

Customized Needs Prompt

Based on your observation of all historical loss weights, the scores and your knowledge about these losses, please develop a new loss weights to train the SR model.

You should follow these rules:

1. The output should in format 'Weights: L1:Perceptual:GAN=??:? (for example: **L1:Perceptual:GAN=1.0:0.1:0.01**)' 'Thoughts: (The reason you give this weights)'.
2. Your ultimate goal is to help SR model achieve a lower score feedback (which indicates a better image quality).
3. You can randomly increase or decrease the weight of each loss by a small amount if historical weights are not enough for making a decision.

LLM's Feedback

Based on the historical data and the goal of improving image quality (lower score), here's a proposed set of updated loss weights for your SR model:

Weights: L1:Perceptual:GAN=0.7:0.3:0.05

Thoughts: **Decreasing the L1 loss weight and slightly increasing the Perceptual loss weight seems beneficial based on the observed score changes.** Initially, the model started with a high L1 loss weight, which has been gradually reduced over training steps. **This reduction correlated with improvements in image quality scores.** The slight increase in Perceptual loss weight helps in preserving more perceptual details, further enhancing image quality. GAN loss weight is kept relatively low to **prevent overfitting to the discriminator and maintain visual fidelity.**

This adjustment aims to leverage the learning from historical weight changes, emphasizing a balance that has shown incremental improvements in image quality scores over training steps. Adjusting weights further could be iterative, guided by continued monitoring of image quality feedback during training.

Figure 6. A case study of LossAgent on classical image super-resolution task at 25000 iterations. The optimization objective is NIQE.